Solar Energy Materials & Solar Cells 93 (2009) 1721–1727

Contents lists available at ScienceDirect

Solar Energy Materials & Solar Cells

journal homepage: www.elsevier.com/locate/solmat

The photonic light trap—Improved light trapping in solar cells by angularly selective filters

Marius Peters [a,b,*], Jan Christoph Goldschmidt [b], Thomas Kirchartz [c], Benedikt Bläsi [b]

[a] University of Freiburg, FMF, Stefan Meier Straße 21, D-79104 Freiburg, Germany
[b] Fraunhofer Institute for Solar Energy Systems ISE, Heidenhofstraße 2, D-79110 Freiburg, Germany
[c] Forschungszentrum Jülich, Institut für Energieforschung (IEF-5), Leo-Brandt-Straße D-52428 Jülich, Germany

ARTICLE INFO

Article history:
Received 17 March 2009
Accepted 18 May 2009
Available online 12 June 2009

Keywords:
Photonic crystals
Novel concepts
Solar cell
Scattering

ABSTRACT

A photonic light trap, i.e. a combination of an angularly selective filter and a light scattering process in a solar cell, results in potentially very efficient light trapping. Angularly selective filters are investigated theoretically and experimentally. One of the filters is used to realize a photonic light trap for a thin-film solar cell with amorphous-silicon absorber layer on a roughened superstrate. We experimentally demonstrate that the light absorption in this solar cell is enhanced by 25% in a wavelength range of 700–750 nm. Accordingly, the quantum efficiency of the solar cell demonstrates an increase of 25% in the same wavelength range.

1. Introduction

Light trapping [1] increases the path length of light inside solar cells. This either leads to a higher short-circuit current density J_{SC}, or it allows decreasing the thickness of the cell while maintaining the same J_{SC}. In the latter case the open-circuit voltage V_{OC} is increased as bulk recombination is reduced with decreasing thickness [2]. In both cases, therefore, light trapping improves the solar cell performance.

Light trapping is commonly achieved by structuring the surface of the solar cell [3]. The structure allows multiple reflections at the front surface, which reduce reflection losses. It also increases the path length by changing the direction of the light in the solar cell by refraction. Typically, the light trapping structure is combined with an antireflection coating to decrease front surface reflection losses further. This technique is used for multi-crystalline silicon solar cells with very high efficiencies [4]. The path length enhancement for this technique is in the range of a factor of $L = 10$. However, for solar cells that become thinner and thinner, more efficient light trapping mechanisms are required.

One mechanism suggested here uses scattering of light inside a solar cell. Combining scattering with total internal reflection, a theoretical path length enhancement of a factor $4n^2$ [5–7] is achieved, with n being the refractive index of the material. In the case of a silicon solar cell with $n = 3.5$, the corresponding factor is $L = 4n^2 = 49$.

Proceeding from this idea, we arrive at the photonic light trap. Very efficient light trapping is possible by combining a scattering mechanism with an angularly selective filter [8–10]. The angularly selective filter restricts the angular acceptance range θ of the system. For the scattered light inside the medium, an effect similar to total internal reflection occurs: All light impinging on the filter with an angle greater than the acceptance angle is trapped. This mechanism achieves path length enhancement with a factor of $1/\sin^2(\theta)$ [11], assuming the Lambertian scattering. Restricting the acceptance angle of the system to the solid angle of the sun, a maximum path length enhancement with a factor $L = 46{,}200$ is possible. This method requires tracking of the solar cell such that the solar illumination always impinges under the same angle. The concept is sketched in Fig. 1.

To realize such a system, two components are required: a scattering mechanism and a suitable optical element. The first component is obtained easily; scattering mechanisms are realized in photovoltaic systems in different ways. Well-known possibilities to achieve scattering include roughening the substrate for thin-film solar cells [12–15] or texturing the backside of a silicon solar cell [16]. With a broader understanding of scattering, we see that the radiative recombination in direct semiconductors (like gallium arsenide) [17] or the emission of light in fluorescent concentrators [18] also fall into this scheme. The difficulties in the realization of a photonic light trap lie in the second component: the suitable optical element.

In this work we experimentally investigate the effect of a photonic light trap on the efficiency of a solar cell. We do this by initially identifying convenient optical elements. The angular

* Corresponding author at: Fraunhofer Institute for Solar Energy Systems ISE, Heidenhofstrase 2, D-79110 Freiburg, Germany. Tel.: +49 761 4588 5148; fax: +49 761 4588 9250.
E-mail address: marius.peters@ise.fraunhofer.de (M. Peters).

0927-0248/$ - see front matter © 2009 Elsevier B.V. All rights reserved.
doi:10.1016/j.solmat.2009.05.019

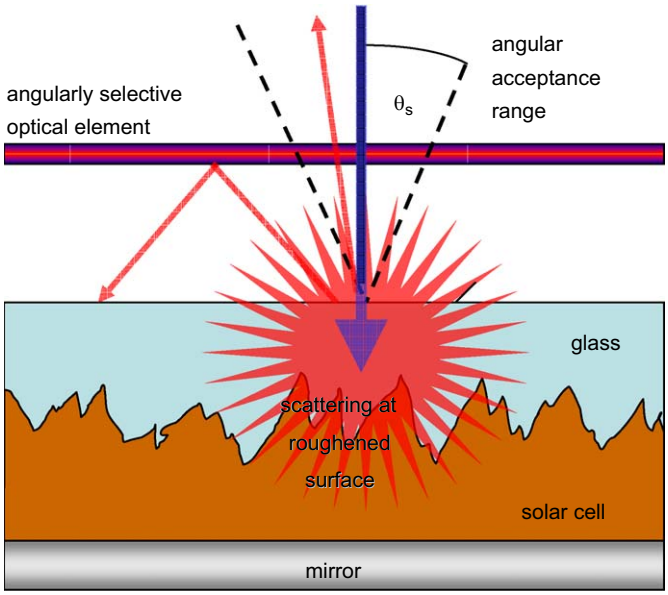

Fig. 1. Schematic sketch of the photonic light trap. The principle of this concept is a combination of angular confinement and a diffusion of radiation. The angular confinement is achieved by an angularly selective optical element. This element is characterized by an angle θ_s, which defines the angular acceptance range of the element. Only light within the angular acceptance range shall be allowed to traverse the filter, all other light shall be reflected. Incident light passes the optical element, enters the PV system and is directionally randomized. In the figure the randomization is realized by a roughened surface; however, many different scattering processes are possible. Only light scattered into the angular acceptance range of the filter may leave the PV system; all other light is trapped.

selectivity of different photonic structures is investigated experimentally and theoretically. The angularly dependent reflection characteristic is described and the Bragg effect is identified as the constituting phenomenon creating angular selectivity. Following that, we will sketch how the Bragg effect is used to create an angularly selective filter with a convenient characteristic. One of the investigated filters will be chosen to realize a photonic light trap for a thin-film solar cell of amorphous silicon. This system will be investigated concerning the absorption in the solar cell and its quantum efficiency. An enhancement of both of these quantities will be found, demonstrating the effect of the photonic light trap.

2. Angular selective filters

The desired characteristic for an angularly selective filter is a transmittance of $T = 1$ in an angular acceptance range between perpendicular incidence and a critical polar angel θ_c, and a reflectance of $R = 1$ for all other angles. The characteristic should show no dependence on the azimuth angle and the wavelength of the light. A filter with this characteristic, however, is not currently known. To attenuate the demands on the filter, the angular selectivity can be restricted to a certain spectral range. As the concept aims towards an increased absorption, it is sensible to chose a spectral region in which the solar cell material absorbs only weakly, i.e. it has a small absorption coefficient. This region of low absorption is typically close to the band edge [8]. For all other wavelengths, the filter needs to be transparent. This characteristic has the advantage that the filter is transparent for diffuse light, which is also used by solar cells. It has been shown that among photonic crystals, filter systems with the desired characteristics can be found. Examples are the rugate filter [19] and the opal.

Several mechanisms exist that result in an angularly dependent reflection in optical filters. In this work we concentrate on photonic crystals, i.e. systems that are described by a spatial periodical function of the refractive index. A given optical characteristic of such a system shows a blue shift for increasing angles of incidence. The reason for this may be explained illustratively by the reflection of a Bragg stack. A Bragg stack shows high reflection, if the Bragg condition

$$\lambda_0 = 2\,dn \tag{1}$$

is satisfied. In this equation, d is the thickness of a layer, λ_0 is the wavelength for which high reflection occurs, and n is the refractive index of the system. The condition as it is written here is valid for normal incidence on the Bragg stack. If the direction of incidence is changed from normal incidence to incidence under an angle α, the Bragg condition is satisfied for

$$\lambda_0(\alpha) = 2d\sqrt{n^2 - \sin^2(\alpha)} \tag{2}$$

This effect is well known. For photonic crystals, it has been described e.g. in [20]. As may be seen from Eq. (2), the Bragg condition is shifted towards the blue for increasing angles of incidence. This principle can be generalized from Bragg stacks to arbitrary 1D periodic systems, and even to more complex periodic systems (3D photonic crystals), within limits.

We now want to use this effect for a path length enhancement in a solar cell. For this purpose we will concentrate on the spectral range where the solar cell is limited by absorption. This spectral range depends on the band edge of the material and the thickness of the solar cell in question. For a simple slab of silicon without further light trapping, the range of low absorption starts at a wavelength of around $\lambda = 1000$ nm for a slab with a thickness of $d = 200\,\mu$m but starts at $\lambda = 520$ nm for a slab with a thickness of $d = 1\,\mu$m. The spectral area of high reflectivity must be positioned so that the reflection losses produced by the filter are negligible. On the other hand, as much light as possible must be trapped in the solar cell. This can be done by designing the filter in such a way that the Bragg reflection for normal incidence is located at energies just underneath the energy range for which increased absorption is desired. This is typically the case for energies in which only a small fraction of the light is absorbed. Let the wavelength above which the filter reflects be λ_0. Light with higher wavelengths cannot be used by the solar cell anyway, as it will not be absorbed, so there are no additional losses under normal conditions. Light with lower wavelengths traverses the filter and enters the solar cell as shown in Fig. 2.

Inside the solar cell the light is scattered, impinging therefore on the filter with a certain angular characteristic. As the reflection of the filter is shifted towards the blue with higher angles of incidence, light with the same wavelength is now reflected if it impinges on the filter with a sufficiently large angle. As can be seen from Fig. 2, the critical angle above which light is reflected is smaller, the closer the wavelength is to λ_0. The filter is, therefore, very effective close to this wavelength λ_0, and therefore especially for light which is poorly absorbed.

The demand on the reflection characteristic of the filter can be easily satisfied under practical conditions, as the position of the reflection peak is defined only by the period length of the filter and may therefore be adjusted by scaling this period length. We will now give a short introduction to two kinds of filters, the Bragg-like filter and the opal, which show the described characteristics.

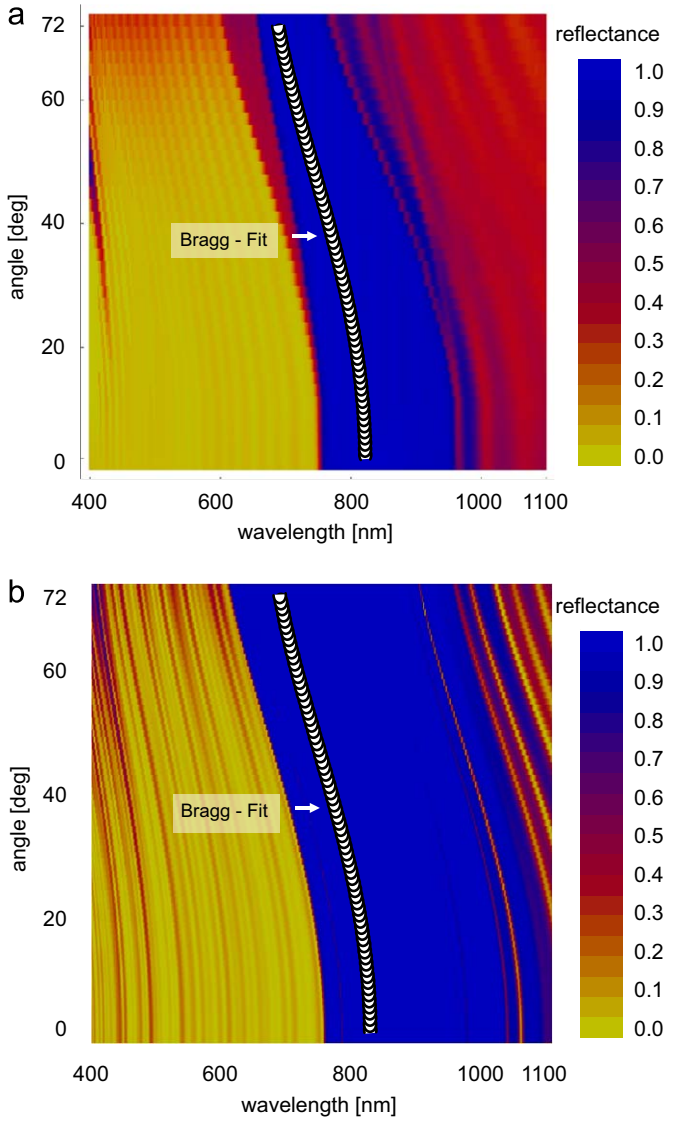

Fig. 2. (a) Simulated and (b) measured angularly dependent reflection characteristic of a band edge filter with a reflection edge at $\lambda = 760$ nm. The filter shows the expected blue shift and the desired angular-dependent reflection for wavelengths below 760 nm. The simulated filter consists of two materials with $n_1 = 1.5$ and $n_2 = 2.0$ and was optimized using an evolutionary algorithm. The filter used for the experiment was fabricated by mso Jena. The angular dependence of the reflection edge was fitted using Bragg's equation with $\bar{n} = 1.75$ and a period of $d = 237.5$ nm for both cases.

2.1. Bragg-like filters

Bragg filters typically consist of two materials with the refractive indices n_1 and n_2 that are ordered periodically. If the Bragg condition for the period d

$$d = \frac{\lambda_0}{2\,\bar{n}} \tag{3}$$

is satisfied, where $\bar{n}$ is the average refractive index, the filter shows an area of high reflectance λ_0 for normal incidence. For arbitrary incidence, the angular dependence of the area of high reflectance is given by

$$\lambda_0(\alpha) = 2d\sqrt{\bar{n}^2 - \sin^2(\alpha)} \tag{4}$$

The simple Bragg stack is typically unsuitable for PV applications, as it shows undesirable reflections caused by harmonics and sidelobes. Several possibilities exist to overcome these inconveniences. One is to use a continuous refractive index profile instead of a discrete one. An example here is the optimized rugate filter, which is based on a sinusoidal refractive index profile [21]. It has already theoretically been shown that with this kind of filter, effective light trapping is possible [19]. Another possibility is to go to a non-periodic discrete refractive index profile. The interference between a great number of layers with different thicknesses may be used to create a large variety of possible reflection characteristics [22]. Even if those filters cease to be periodical, the principle, that high reflectance is caused by constructive interference between the waves reflected at each layer still holds. This principle has the effect that also the angular characteristic described in Eq. (4) remains mostly valid.[1] The characteristic of a non-periodic band edge filter is given in Fig. 2.

For the simulation of the filter, the approach of characteristic matrices has been used [23]. The simulated filter was optimized using an evolutionary algorithm developed for this purpose. The filter used for the experiments was fabricated especially for us by Mso Jena according to our specifications. The measurement of the angular-dependent reflection characteristic was performed using a goniometer and a Fourier spectrometer.

From Eq. (4), the spectral range for which angular selectivity occurs may also be obtained. It is clear that the angular dependence becomes more pronounced as the average refractive index of the filter becomes smaller. As typical materials used for Bragg-like filters have a refractive index between $n_1 = 1.5$ and $n_2 = 2$, typical values for $\bar{n}$ are around 1.75. The variation δ of the wavelength possible with such a filter is

$$\delta_{\max} = \frac{\lambda_0(0^\circ)}{\lambda_0(90^\circ)} = 1.22 \tag{5}$$

This means that for a reflection peak starting at $\lambda_0 = 1000$ nm the light trapping covers a spectral range of $820\,\text{nm} < \lambda < 1000\,\text{nm}$.

2.2. Opal

The second filter investigated is the opal. The opal is a three-dimensional photonic crystal consisting of spheres ordered in the face-centered cubic (fcc) structure. The optical characteristics of the opal are well known and described elsewhere [24]. At this point, it is sufficient to know that an opal has several reflection bands that occur for different wavelengths and are caused by interference between the sphere layers. These reflection bands are described by a band structure. The gap, we want to concentrate on, is the one between the 2nd and the 3rd band in the growth direction of the opal ($\langle 111 \rangle$ direction in Miller indices). The angular dependence of the reflection peak for an opal is given by

$$\lambda_{111}(\alpha) = 2d_{111}\sqrt{n_{eff}^2 - \sin^2(\alpha)} \tag{6}$$

In this equation, d_{111} denotes the distance between two layers of spheres in the $\langle 111 \rangle$ direction. If the sphere diameter is given by D, this distance is given by

$$d_{111} = \sqrt{\frac{2}{3}}D \approx 0.816\,D. \tag{7}$$

The effective refractive index of the opal is denoted n_{eff}. In the closest package 74% of the volume is filled with spheres, while 26% are air voids. A typical sphere material is polymethylmethacrylate

[1] It is possible to create optical elements for which the angular characteristic is changed. It is especially possible to use the method presented in [20] to create elements with a distinctive angular characteristic. However, a spectral range of high reflectance is created by constructive interference and a high magnitude is created by many reflections that interfere constructively. Many filters with a spectrally selective reflectance are therefore close to periodic systems and are described in an adequate way by Eq. (4).

(PMMA) with a refractive index of $n \approx 1.5$. This results in an effective refractive index of the opal of $n_{eff} = 1.37$. In real opals, the effective refractive index must be considered to be a little lower because of imperfections in the sphere stacks.

Eq. (6) is only valid up to a certain point. The reason for this is that when changing the angle of incidence α, the crystallographic orientation of light relative to photonic crystal is changed. If the relevant direction for the interference changes from the $\langle 111 \rangle$ direction to another crystallographic orientation with another period, Eq. (6) no longer describes the angular-dependent reflection. We have performed simulations and experiments that show that for typical opals with a finite thickness, Eq. (6) provides a good description of the angular characteristic for angles up to 70° (cf. Fig. 3).

The opals used in the experiments were produced by L. Steidl at the University of Mainz. These crystals consisted of ca. 10 layers of spheres with a sphere diameter of $D = 255$ nm and a total thickness of 2.1 μm. A measurement of the angularly dependent reflectance was performed using a goniometer and a Fourier spectrometer. Additionally, we have performed simulations using the RCWA method [25,26]. The results of the simulations and measurements are shown in Fig. 3.

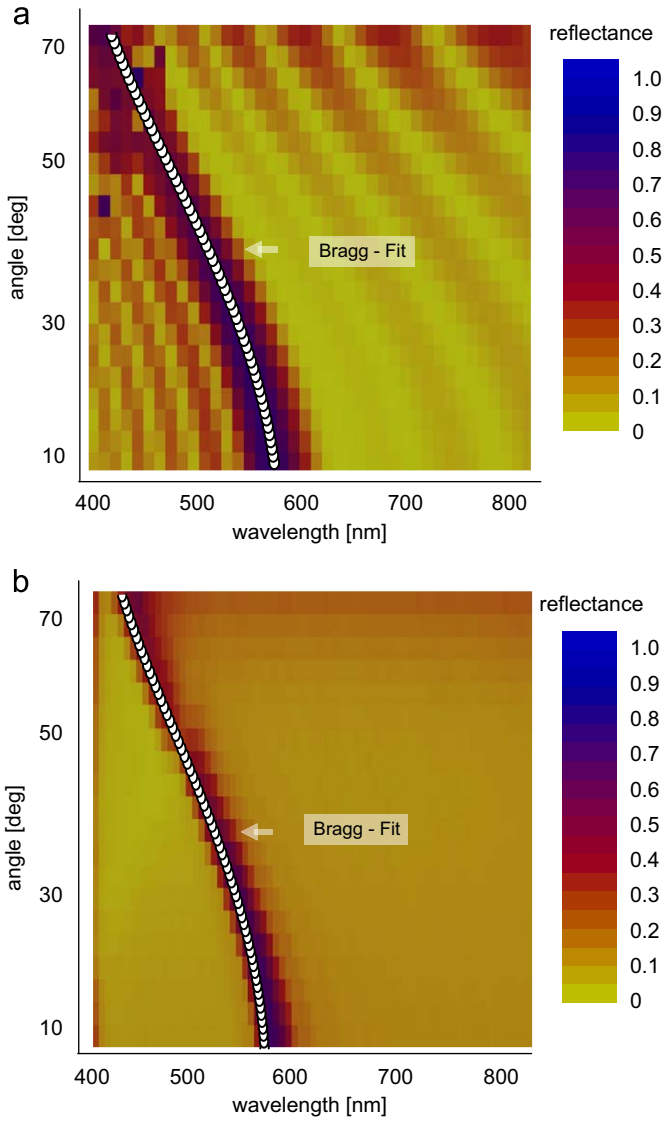

Fig. 3. (a) Simulated and (b) measured angular-dependent reflection characteristic of an opal. The opal was fabricated at the University of Mainz. It consists of 10 layers of spheres made of PMMA with a diameter of 255 nm and a refractive index of $n \approx 1.5$. The position of the reflectance peak was fitted using Bragg's formula with $d_{111} = 208.1$ nm and $n_{eff} = 1.36$.

3. Experiments

In this section, we show that the quantum efficiency of a thin cell of amorphous silicon is increased in the region of the blue shift of a photonic structure and that this increase is caused by an absorption enhancement. We start with an experiment showing an increased absorption in the solar cell and proceed to measurements of the quantum efficiency.

In previous works, theoretical examinations using optimized rugate systems as angular selective filters yielded a predicted absolute efficiency increase of 1.5% for a silicon solar cell [19]. An increased absorption in a thin silicon wafer has also been shown experimentally [8].

3.1. Absorption enhancement

To examine the absorption enhancement, we used a band-edge filter with a characteristic similar to the one shown in Fig. 2. The filter was designed especially for the application on an amorphous silicon thin-film solar cell and had a reflection peak that started at $\lambda = 760$ nm for normal incidence. Looking at Eq. (5), we expect an effect of the filter between $630\,\text{nm} < \lambda < 760\,\text{nm}$. The used solar cell was an amorphous silicon solar cell on a roughened glass superstrate [12] fabricated at FZ Jülich. Because of the rough superstrate, the light is scattered directly by cell and superstrate. This scattering assures the diffusion of the internal radiation.[2] Additionally, a silver reflector is deposited on the rear surface of the cell to increase the back reflection. The region of low absorption for this cell starts at $\lambda \approx 750$ nm.

To obtain the absorption of the cell we performed measurements of the reflection and transmission characteristics. These measurements were performed using a photospectrometer (Varian Cary 500*i*) combined with an integrating sphere to detect the direct and the diffuse radiation. We measured the spectral reflectance R_{cell} and transmission T_{cell} of the cell system (cell on substrate+silver reflector) alone. As the cell system showed no transmission at all in the spectral region of interest, the reflectance is a direct measure of how much light is absorbed in the cell system A_{cell}:

$$A_{cell} = 1 - R_{cell} \tag{8}$$

The results of this measurement are shown in Fig. 4. Subsequently, we measured the reflection of the cell system with each of the filters placed on top of the cell system. The filters had been deposited on BA7 glass substrates. Independently from the characteristics of the filters, this causes additional reflection losses from the air glass interface. However, in a later photovoltaic module, the filter may be deposited directly on a covering glass. This allows one, therefore, to estimate the potential of the light trapping concept on a module level. Therefore, we also measured the cell system with a covering glass. As the absorption of filter and covering glass are negligible in the spectral region of interest, the obtained absorption is that of the solar cell. The results of these measurements are also shown in Fig. 4.

Fig. 4a shows the obtained absorption. A positive effect of the filter is noticeable between $\lambda = 675$ and 750 nm. However, this onset of positive effect occurs at longer wavelength than expected from Eq. (5). This is not very surprising, as the effect of angular

[2] Internal radiation here refers to radiation in the photonic light trap, i.e. below the filter.

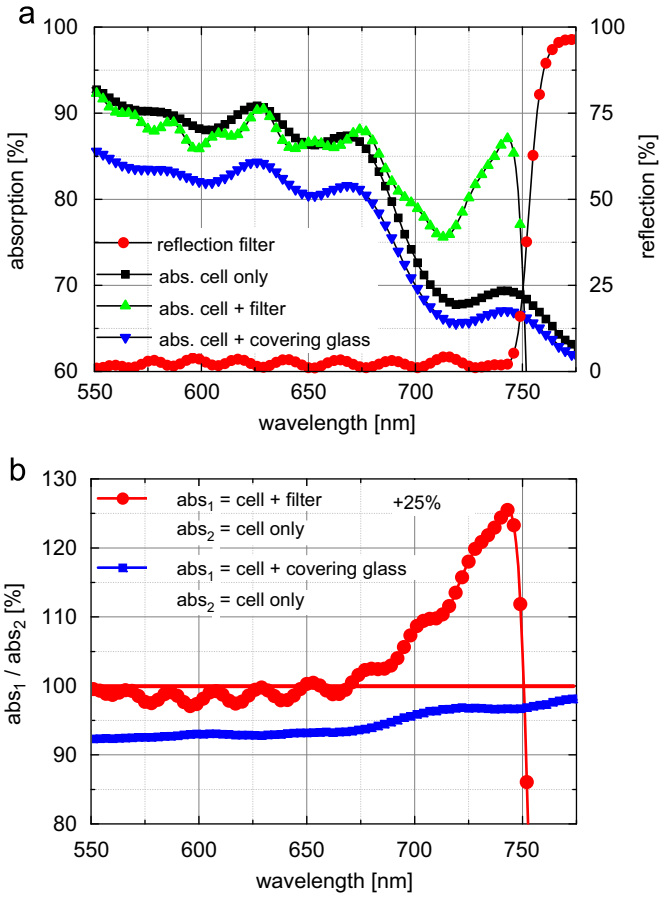

Fig. 4. (a) Absorption obtained from experiments for the cell system only (black squares), the cell systems with the band-edge filter placed on top (green triangles) and with the cover glass (blue triangles). Additionally shown is the reflection of the filter (red dots). (b) Relative change in absorption. Shown are the changes for a system with filter relative to the cell only (red dots) and a system with covering glass (blue squares). The relative absorption is increased up to 125%.For interpretation of the references to colour in this figure legend, the reader is referred to the to the web version of this article.

confinement for the smaller wavelengths is comparably weak and they are absorbed more strongly anyway. Above $\lambda = 750$ nm the reflection of the filter sets in and the absorption of the systems with filter is reduced to practically zero. The relative absorption increase is displayed in Fig. 4b. The red dotted curve shows the relative change in absorption of the cell systems with filter on top compared to the cell without. For wavelengths below $\lambda = 650$ nm, the absorption is slightly reduced because the attached filter causes reflection losses. However, above $\lambda = 675$ nm an increased absorption is noticeable due to the effect of the photonic light trap. The increase is higher, the closer the wavelengths come to the reflection peak. A maximum value of 125% is reached for a wavelength of $\lambda = 745$ nm. The blue squared curve shows the relative absorption between cells with covering glass and cells without. For all wavelengths, the absorption is reduced for the system with covering glass because of the reflection losses. Comparing the red and the blue curve, a positive effect for the photonic light trap is noticeable for all wavelengths.

As noted previously, the absorption in the filter and in the cover glass are negligible, so the observed change in the absorption is a change in the absorption of the cell. With this measurement we showed that the absorption is considerably increased by the application of the photonic light trap. Now, we examine the effects of this enhancement on the quantum efficiency of the system.

3.2. Enhancement of the quantum efficiency

In a second set of measurements, the external quantum efficiency (EQE) was measured for the same systems. The results of these measurements are shown in Fig. 5. Fig. 5a shows the external quantum efficiencies for the systems cell only, cell+filter and cell+covering glass. Also given is the reflection of the filter. Because of reflection losses, the system with covering glass shows the lowest EQE for all wavelengths. The filter shows less reflection losses and the EQE for the system with filter is higher than the one for the system with covering glass for all wavelengths. For wavelengths between 640 nm $< \lambda <$ 740 nm, the EQE for the system with filter is even higher than the one for the cell only. This corresponds to the results of the absorption measurements and also to the result of Eq. (5). It must be emphasized that the filter still produces reflection losses in this spectral region. However, the increased quantum efficiency shows that the positive effects of the photonic light trap overcome the negative ones.

The ratios of the EQEs between the systems cell+filter/cell only and cell+covering glass/cell only are given in Fig. 5b. The form of the curves is similar to the ones for the absorption enhancement

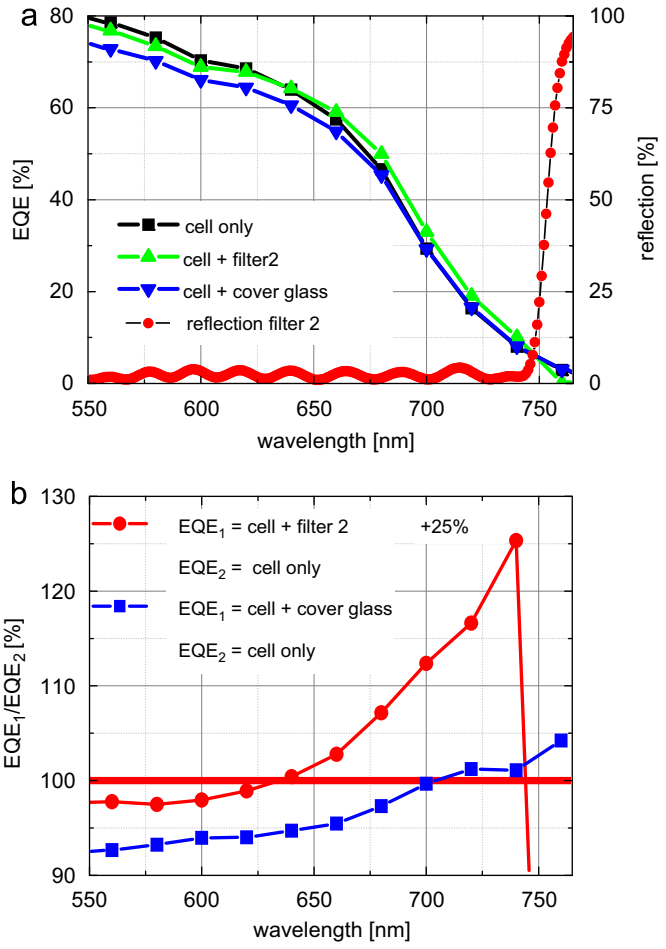

Fig. 5. (a) Measured quantum efficiency for the cell system only (black squares), the cell system with one of the filters (green triangles) and the cell system with a covering glass (blue triangles). Also given is the reflection of the filter (red dots). For wavelengths greater than $\lambda = 650$ nm, the system with filter shows a quantum efficiency that is higher than for the system without, even though the filter produces reflection losses here. In (b) Ratio between the quantum efficiencies between the system with filter and without filter (red dots) and between the system with filter and with cover glass are shown (blue triangles). The quantum efficiency is increased up to 25%. For interpretation of the reference to colour in this figure legend, the reader is referred to the web version of the article.

Table 1
Comparison of the integrated quantum efficiencies for the systems solar cell, solar cell+filter and solar cell+covering glass.

	Solar cell+covering glass (%)	Solar cell+filter (%)	Solar cell only (%)
Compared to: solar cell+covering glass	100.0	104.4	107.9
Compared to: solar cell+covering glass weighted with AM 1.5	100.0	105.5	108.0

In the first column, the comparison is given with respect to the solar cell only. The reduced values for the other systems here are caused by reflection losses. In the second column, the comparison is with respect to the solar cell+covering glass. The improved performance for the system with filter is caused by a higher transmission of the filter compared to the covering glass and the photonic light trap. In columns three and four, the integrated EQE is additionally weighted with the AM 1.5 spectrum. Taking this into account, the performance of the light trap is additionally slightly improved.

in Fig. 4b, and the maximum value of an enhancement of 25% is also similar. This shows that the absorption in a thin cell of amorphous silicon is increased up to more than 25% by the photonic light trap, and that this increased absorption is transferred to an increased quantum efficiency.

One interesting point about Fig. 5b is that the system cell+covering glass also shows a higher quantum efficiency than the cell only for wavelengths greater than $\lambda = 700$ nm. This effect may also be observed in Fig. 4b, though in an attenuated form. The increased absorption and quantum efficiency here is explained by the Fresnel reflections that also show an angular dependence.

It must be said that the solar cell alone showed the best performance when compared to a system of solar cell+filter or solar cell+covering glass. This is because filters and covering glass induce reflection losses. These losses affect all wavelengths and are at present not overcome by the gain produced by the angularly selective filter. However, the performance of the system cell+filter was improved when compared to the system cell+covering glass (Table 1).

4. Summary

In summary, we have investigated and characterized a system which we call the photonic light trap. The principle of the photonic light trap is a combination of angular confinement and a scattering process which results in a trapping of the internal radiation. We have started to characterize optical elements which provide angular confinement. Two kind of optical filters were investigated in particular, the Bragg-like filter and the opal. For both kinds of filters, the angularly dependent reflection characteristic was investigated by numerical simulations and by experiment. The Bragg effect was identified as the principle creating angular selectivity for the filters presented, and we have discussed how this effect may be used to form a photonic light trap. The band edge filter, a Bragg-like system, was used to realize a photonic light trap for a thin-film solar cell of amorphous silicon. For this system an increased absorption of up to 25% was demonstrated. Subsequently, measurements of the quantum efficiency of the same system were performed. These measurements showed that the increased absorption is transferred into increased quantum efficiency. For the quantum efficiency as well, an increase of up to 25% was demonstrated. Finally, the integrated quantum efficiency weighted with the AM 1.5 spectrum was calculated. The result of this calculation was that the efficiency of the photonic light trap was decreased 2.5% compared to the solitary solar cell because of reflection losses. However, compared to the system with a covering glass the efficiency was increased by 5.5%. This enhancement can be expected if the filter is deposited directly onto a comparable solar module. These results show that it is possible to improve PV systems by means of angular confinement.

Acknowledgments

We thank the DFG for their financial support in the project Nanosun (Pak88) and the BMBF for their financial support in the project Nanovolt. Jan Christoph Goldschmidt gratefully acknowledges the scholarship support from the Deutsche Bundesstiftung Umwelt (DBU) and the ideational support from the Heinrich Böll Stiftung and the Studienstiftung des deutschen Volkes. We thank especially Elisabeth Schäffer and Tim Rist for their support in the measurements and Andreas Lambertz (FZ-Jülich) for fabrication of the used a-Si:H solar cell.

References

[1] D. Redfield, Multiple-pass thin-film silicon solar cells, App. Phys. Lett. 25 (1974) 647–648.
[2] R. Brendel, H.J. Queisser, On the thickness dependence of open circuit voltages of p-n junction solar cells, Sol. Energy Mater. Sol. Cells 29 (1993) 397–401.
[3] P. Campbell, M. Green, Light Trapping properties of pyramidally textured surfaces, J. Appl. Phys. 62 (1987) 243–249.
[4] O. Schultz, S.W. Glunz, J.C. Goldschmidt, H. Lautenschlager, A. Leimenstoll, E. Schneider-Lächner, G.P. Willeke, in: Proceedings of the 19th European Photovoltaic Solar Energy Conference, Paris, WIP Renewable Energies, Munich, 2004.
[5] E. Yablonovitch, Statistical ray optics, J. Opt. Soc. Am. 72 (1982) 899–907.
[6] M. Green, High Efficiency Solar Cells, Trans. Tech. Publications, Aedermannsdorf, Switzerland, 1987, pp. 96–97.
[7] M.A. Green, Lambertian light trapping in textured solar cells and light-emitting diodes: analytical solutions, Prog. Photovolt.: Res. Appl. 10 (2002) 235–241.
[8] C. Ulbrich, S. Fahr, J. Üpping, M. Peters, T. Kirchartz, C. Rockstuhl, R. Wehrspohn, A. Gombert, F. Lederer, U. Rau, Directional selectivity and ultra-light-trapping in solar cells, Phys. Status. Solidi A 205 (2008) 2831–2843.
[9] V. Badescu, Spectrally and angularly selective photothermal and photovoltaic converters under one-sun illumination, J. Phys. D: Appl. Phys. 38 (2005) 2166–2172.
[10] A. Goetzberger, J.C. Goldschmidt, M. Peters, P. Loeper, Light trapping, a new approach to spectrum splitting, Sol. Energy Mater. Sol. Cells 92 (12) (2008) 1570–1578.
[11] J.C. Miñano, in: A. Luque, G.L. Araújo (Eds.), Physical Limitations to Photovoltaic Solar Energy Conversion, Hilger, Bristol, UK, 1990, pp. 50–55.
[12] B. Rech, J. Müller, T.S. Repmann, O. Kluth, T. Roschek, J. Hüpkes, H. Stiebig, W. Appenzeller, in: J.R. Abelson, G. Ganguly, H. Matsumura, J. Robertson, E.A. Schiff (Eds.), Amorphous and Nanocrystalline Silicon-Based Films, Material Research Society Symposium Proceeding, vol. 762, 2003, p. 3.1.
[13] T. Tiedje, B. Abeles, J.M. Cebulka, J. Pelz, Photoconductivity enhancement by light trapping in rough amorphous silicon, Appl. Phys. Lett. 42 (1983) 712–714.
[14] V. Terrazzoni Daudrix, et al., Characterisation of rough reflecting substrates incorporated into thin-film silicon solar cells, Prog. Photovolt: Res. Appl. 14 (2006) 485–498.
[15] C. Rockstuhl, S. Fahr, F. Lederer, K. Bittkau, T. Beckers, R. Carius, Local versus global absorption in thin-film solar cells with randomly textured surfaces, Appl. Phys. Lett. 93 (2008) 061105–0611053.
[16] D. Kray, M. Hermle, S.W. Glunz, Theory and Experiments on the Back Side Reflectance of Silicon Wafer Solar Cells, Prog. Photovolt: Res. Appl. 16 (2008) 1–15.
[17] Y.P. Varshni, Band to Band Radiative Recombination in Groups IV, VI and III-V Semiconductors, Phys. Status. Solidi. 19 (1967) 459–514.
[18] A. Zastrow, Physikalische Analyse der Energieverlustmechanismen in Fluoreszenzkonzentratoren, Dissertation, Ùniversität Freiburg, 1981.
[19] S. Fahr, C. Ulbrich, T. Kirchartz, C. Rockstuhl, F. Lederer, Rugate filter for light-trapping in solar cells, Opt. Express 16 (2008) 9332–9343.

[20] G.M. Gajiev, Bragg reflection spectroscopy of opal-like photonic crystals, Phys. Rev. B 72 (2005) 205115–2051159.
[21] W.H. Southwell, Using apodization functions to reduce sidelobes in rugate filters, Appl. Opt. 28 (1989) 5091–5094.
[22] B.T. Sullivan, J.A. Dobrowolski, Optimal single-band normal-incidence anti-reflection coatings, Appl. Opt. 35 (1996) 644–658.
[23] H.A. Macleod, Thin-Film Optical Filters, Adam Hilger Ltd., Bristol, 1986, pp. 17–39.
[24] I.I. Tarhan, G.H. Watson, Photonic Band Structure of fcc Colloidal Crystals, Phys. Rev. Lett. 76 (1996) 315–318.
[25] M.G. Moharam, Formulation for stable and efficient implementation of the rigorous coupled-wave analysis of binary gratings, J. Opt. Soc. Am. A 12 (1995) 1068–1075.
[26] Ph. Lalanne, M.P. Jurek, Diffraction gratings and buried nano-electrodes—architectures for organic solar cells, J. Mod. Opt. 45 (1998) 1357–1374.